frontiers in Materials

ORIGINAL RESEARCH
published: 24 October 2022
doi: 10.3389/fmats.2022.803596

Research on the Phase Transformation of a Newly Developed Carbonitride-Strengthened Martensitic Heat Resistant Steel

Wenfeng Zhang[1,2,3], *Ping Pan*[2]*, *Jun Zhou*[2], *Wei Xiong*[2], *Yunqiang Liu*[2], *Xiaogang Liu*[2,3] and *Wei Yan*[4]*

[1]Guangdong Polytechnic of Water Resources and Electric Engineering, Guangzhou, China, [2]School of Mechanical Engineering, Gulin University of Aerospace Technology, Guilin, China, [3]Guangxi Colleges and Universities Key Laboratory of Robot & Welding, Guilin University of Aerospace Technology, Guilin, China, [4]Institute of Metal Research, Chinese Academy of Sciences, Shenyang, China

The phase transformation behavior of nitrides-strengthened martensitic (NSM) heat resistant steel, showing excellent creep behavior under 500°C, was studied in this article. The results showed that during the heating procedure, the formation of austenite was composed successively by intermetallic compound formation in martensite, crystal structure shift from body-centered cubic (BCC) to face-centered cubic (FCC), martensite/ferrite grain boundary migration, austenite nucleation, and growing. The crystal structure switch from BCC to FCC was sensitive to temperature, while the switch from FCC to BCC was only done with phase transformations. During the continuous cooling procedure, the carbide-free bainite would form if the cooling rate was beneath the critical cooling rate. The critical cooling rate was defined as 0.5°C/s for single martensite in NSM steel, according to its inconsistent results of microstructure and continuous cooling transformation (CCT) expansion curve under this condition. Two phase transformation zones were detected in NSM steel: one was a nose-shaped bainite zone and the other was a stripe-shaped martensite zone.

Keywords: phase transformation, carbon-free bainite, CCT diagram, martensitic heat resistant steel, nitrides strengthened

OPEN ACCESS

Edited by:
Zengbao Jiao,
Hong Kong Polytechnic University, Hong Kong SAR, China

Reviewed by:
Pavlo Maruschak,
Ternopil Ivan Pului National Technical University, Ukraine
Xue Hu,
Shihezi University, China

***Correspondence:**
Ping Pan
PP5648349@163.com
Wei Yan
weiyan@imr.ac.cn

Specialty section:
This article was submitted to Structural Materials, a section of the journal Frontiers in Materials

Received: *28 October 2021*
Accepted: *17 January 2022*
Published: *24 October 2022*

Citation:
Zhang W, Pan P, Zhou J, Xiong W, Liu Y, Liu X and Yan W (2022) Research on the Phase Transformation of a Newly Developed Carbonitride-Strengthened Martensitic Heat Resistant Steel. Front. Mater. 9:803596. doi: 10.3389/fmats.2022.803596

INTRODUCTION

The large $M_{23}C_6$ carbides in the martensitic heat resistant steel contribute to the pining effect of retarding boundaries and subboundaries migration (Kipelova et al., 2011). Therefore, the $M_{23}C_6$ carbides could efficiently delay or even eliminate the recrystallization if there are enough of them (Rojas et al., 2011). Yet the other kind of precipitates, the tiny MX particles, could only increase the Zenor pining pressure and have no obvious benefit on prevent the recrystallization (Sawada et al., 2001). However, the 9-12Cr heat resistant steel with a high density of MX particles and very rare $M_{23}C_6$ displayed a far better creep resistant property than those that contain a high density of $M_{23}C_6$ particles (Wang et al., 2017). Therefore, the exploration of this type of nitrides-strengthened martensitic (NSM) heat resistant steel, containing a high density of MX particles and very rare $M_{23}C_6$, gained lots of interest. A new kind of processing procedure, high temperature deformation associated with heat treatment, of this steel as well,

as its deformation behavior and the precipitation character, were studied in the earlier research (Zhang et al., 2011; Zhang et al., 2012; Zhang et al., 2014a; Zhang et al., 2014b; Zhang et al., 2015).

The phase transformation, especially the phase transformation during cooling, determines the final microstructure and mechanical properties of the steels. Therefore, many researchers focused on the transformation of super-cooled austenite, especially the martensite and bainite transformation. Three different kinds of martensite transformation occurred under different conditions. Non-isothermal martensite transformation, unlike isothermal martensite transformation and explosive martensite transformation, is the most common one, happening in a continuous cooling procedure and finishing in seconds (Xu, 1999a). However, the bainite transformation found usually occurred during isothermal holding procedure and was very sensitive to temperatures. In addition to upper bainite and lower bainite, the granular bainite is rare and forms at a higher temperature (Xu and Liu, 1991). Therefore, the transformation of super-cooled austenite transformation is basic and crucially important for all the metals. On the other hand, the phase transformation during heating process was not given enough attention, although it was also crucial to optimize the microstructure and properties. It was assumed that the austenitization during heating determines the basic characteristics of microstructure through influencing grain size, contents of solid solution elements, and volume of unsolved particles (Law and Edmonds, 1980; Speich et al., 1981; Tokizane et al., 1982).

The alloy elements affect the phase transformation greatly, especially the solid solution atoms, such as carbon and nitrogen, due to their strong effect of solution strengthening. Like carbon, the solid solution nitrogen atoms would lower the A_3 temperature and stabilize the austenite. Therefore, the solution nitrogen would postpone the transformation of austenite to martensite, while promoting the transformation of martensite to austenite. However, the nitrides, usually NbN compounds, would form in the austenite and the nose temperature of nitrides precipitation was around 920°C. Although the nitrides content of 980°C-austenized situation, which was the optical annealing procedure for nitrides-strengthened steel, was smaller than 920°C-austenized situation, a great deal of solid solution nitrogen in the 980°C-austenized specimen was consumed. At the same time, the formation of nitrides also consumed most of the solid solution Nb atoms. Compared with the carbides-strengthened heat resistant steel, the nitrides-strengthened steel had a higher A_3 temperature and the stability of austenite was worse. Most research focused on the austenite nucleus from different primary phases such as pearlite, martensite, bainite, and duplex phases during heating process (Law and Edmonds, 1980). However, little research has focused on the occurrence of crystal structure change and the role it plays in the formation of autenite. Therefore, this paper focused on the phase transformation during continuous heating and cooling processes. It could enrich the data base of NSM steel and accelerate its development. Moreover, the isothermal holding experiment over 700°C might provide primary data for the microstructure evolution during service above 700°C conditions.

EXPERIMENTAL PROCEDURE

The steel was melted in a 25 kg vacuum induction melting furnace. The chemical composition of carbonitrides-strengthened heat resistant steel is listed in **Table 1**. The contents of elements, except N, S, and O, that were obtained from the gas analysis were tested by chemical analysis. Bars for the continuous cooling test were cut from the ingot and then machined into bars of 3 mm diameter and 10 mm gage length, with a blind hole of 2 mm diameter and 10 mm length in the center of one side.

Two groups of specimens, Groups A and B, were prepared through different schedules listed in **Table 2**. All the specimens in Group A were isothermal held for 5 min at 980°C with different heating rates of 0.1°C/s, 1°C/s, 2°C/s, and 5°C/s. Then, they were cooled down to room temperature at 1°C/s. Group B specimens cooled down at different cooling rates of 5°C/s, 2°C/s, 1°C/s, 0.1°C/s, 0.05°C/s, and 0.02°C/s, after they were heated up to 980°C at 1°C/s, and isothermal holding for 5 min.

The dilatation coefficient was tested by a Formaster-F thermodilatometry, while the micro-hardness was carried on by a Wilson Wolpert 401 MVD digital micro-hardness tester. The microstructures of NSM steel specimens were observed under a BX41MOLYMPU optical microscope (OM), a TESCAN3SBH scanning electron microscope (SEM), and a Phillips TECNAI20 transmission electron microscope (TEM).

RESULTS

Effect of Heating Rate on High Temperature Austenite Stability

The microstructures of specimens, up-heated to 980°C at different heating rates and cooled down at 1°C/s, were all consisted of martensite, as shown in **Figure 1** and showing no distinct difference. But when up-heated at 1°C/s, the lath martensite character was more obvious, and the width of martensite lath became larger.

Normally, the austenite transformation took place at a higher temperature when the heating rate was higher, due to transformation hysteresis. But the austenite transformation, along with the Curie point, in NSM steel exhibited a deviation from the track at the heating rate of 2°C/s, as shown in **Table 3**. The lowest austenite transformation temperature started at 745°C and finished at 845°C with the heating rate of 2°C/s, while the highest temperature started at 860°C and finished at 950°C with the heating rate of 1°C/s. The Curie point temperature was accordant with austenite transformation temperature.

Microstructures at Different Cooling Rates

After thermal holding for 5 min at 980°C, which ensured the microstructure fully austenized, the NSM steel specimens were cooled down to room temperature at different rates. With the cooling rates raised up to 1°C/s from 0.02°C/s, the martensite-bainite double phase microstructure evolved into martensite single phase, as shown in **Figure 2**. The acicular bainite, indicated by the red arrows, mainly remained perpendicular to martensite lath, tagged in blue arrows, as shown in **Figures 2A,B**.

TABLE 1 | Chemical composition of the NSM steel in wt%.

Elements	C	Si	Mn	Cr	W	V	Nb	N	S	P	O
Content	0.017	0.09	1.23	9.18	1.40	0.14	0.058	0.035	0.003	0.005	0.010

TABLE 2 | The heat treatment procedure of experimental steels.

Steels	Heating rate, °C/s	Cooling rate, °C/s
Group A	0.1/1/2/5	1
Group B	1	5/2/1/0.1/0.05/0.02

TABLE 3 | The transformation points of the NSM steel when heated at different rates.

Heating rates, °C/s	0.1	1	2	5
Curie point, °C	670	775	625	750
A_{c1}, °C	790	860	745	860
A_{c3}, °C	860	950	845	940

However, the acicular bainite grew wider when the cooling rate raised to 0.1°C/s, some of which even showed convex lens shapes, as shown in **Figure 2C**. Meanwhile, the micro-hardness of the microstructure increased from 192HV to 291HV, listed in **Table 3**. Although the acicular bainite width increased, the microstructure hardness increased by 100HV, while the marginal difference between 0.1°C/s-microstructure and 1°C/s-microstructure was only 20HV. As illustrated in **Figure 2D**, the 1°C/s-microstructure was single martensite, which meant the lens-shaped bainite had higher hardness value than the acicular ones. When the cooling rates went beyond 1°C/s, the microstructure showed no distinct differences, which were mainly consisted by lath martensite.

The CCT Curves

With the temperature increasing, one or several atoms in the crystal lattice would shuffle to a lower energy barrier location. This would in turn regain the lattice symmetry. This change in the linear expansion curve was characterized as the Curie point of ferromagnetism. As shown in **Figure 3**, the Curie point appeared before the austenite transformation.

The dilation curve of the heating process indicated the occurrence of the Curie point of ferromagnetism, which was caused by the point group asymmetry. According to Neumann's Principle, this asymmetry was caused by the atoms' movement, which was called "shuffle" in the 1970s by former researchers (Xu, 1999b). On the other hand, the martensite-austenite transformation was a type of displacive phase transformation, which was also associated with the atoms movement-"shuffle". And the atom movement would not stop until the BCC-FCC crystal structure change completed. Therefore, the Curie point of ferromagnetism occurrence indicated that the movement of atoms had already started. And the atom movement would cause the change of crystal structure.

Meanwhile, the Curie point of ferromagnetism indicated that it was sensitive to the heating rate from tests results. But it could

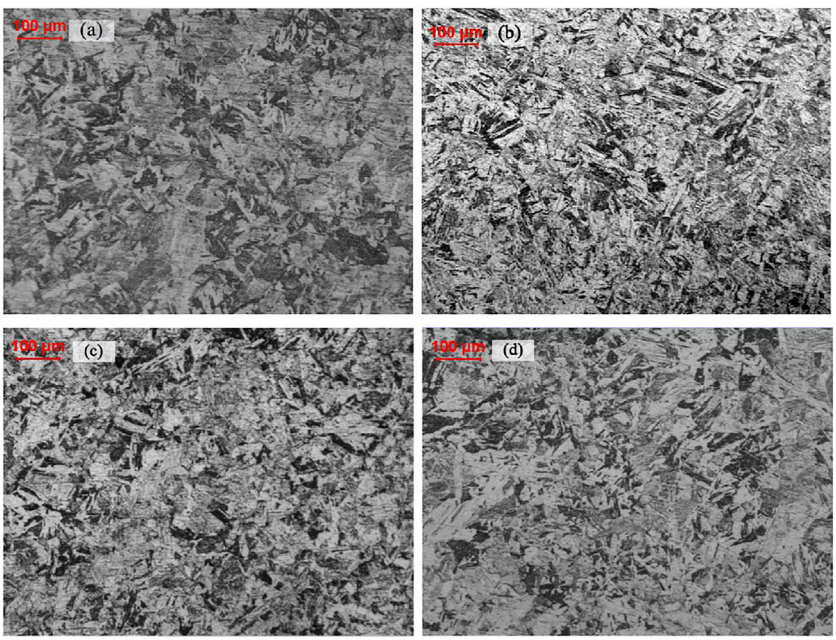

FIGURE 1 | Microstructure of Group A NSM steel specimens heated at different rates of **(A)** 0.1°C/s, **(B)** 1°C/s, **(C)** 2°C/s and **(D)** 5°C/s.

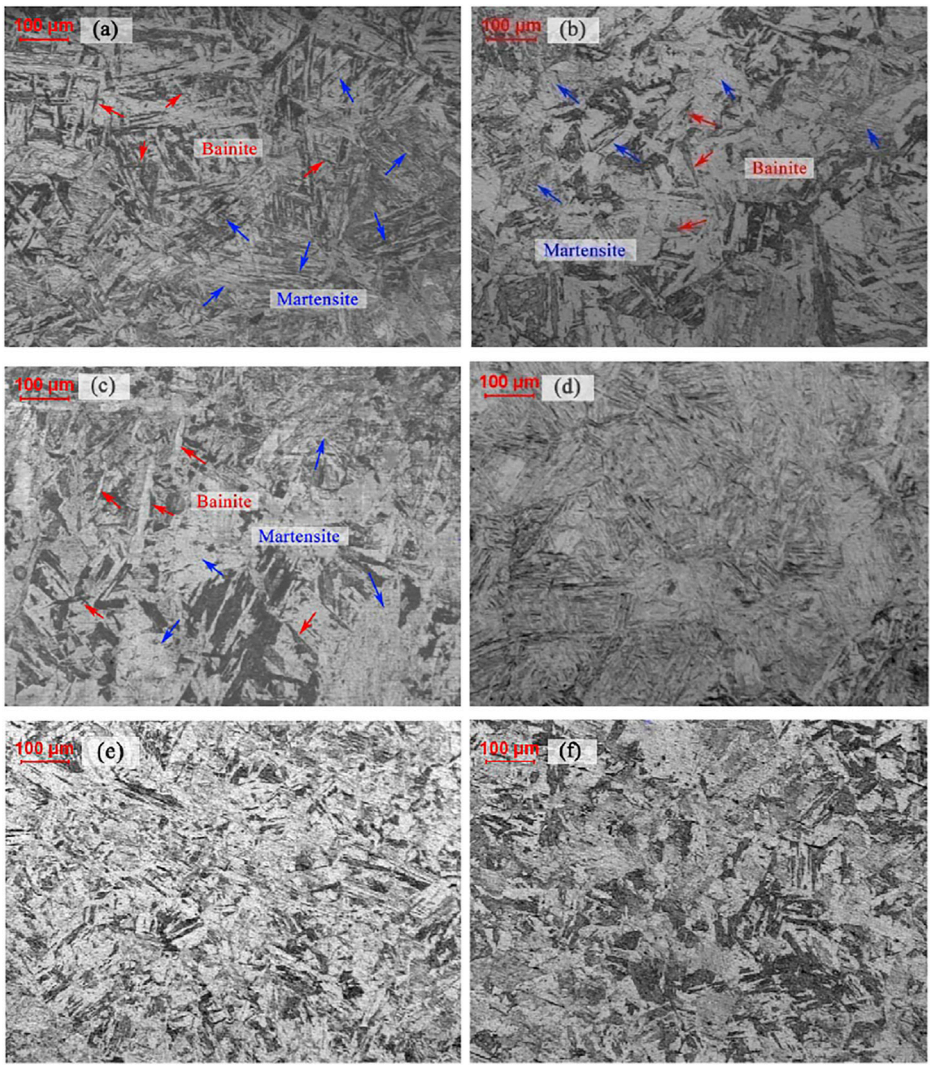

FIGURE 2 | Microstructure of group B NSM steel specimens isothermally held for 5 min with a cooling rate of **(A)** 0.02°C/s, **(B)** 0.05°C/s, **(C)** 0.1°C/s, **(D)** 1°C/s, **(E)** 2°C/s and **(F)** 5°C/s.

not exclude the possibility that the difference of Curie point of ferromagnetism temperature might be caused by the degree of superheat, like the degree of supercooling in crystallization. The test results might be different if the heating rate/cooling rates were different, although the Curie point of ferromagnetism/crystallization temperature were specific. But it could be certain that BCC-FCC transformation was sensitive to temperature.

Therefore, the Curie ferromagnetism occurrence before the phase transformation indicated that some atoms in BCC had ready moved to a stable place and converted the crystal structure into FCC, before the austenite nucleation. The austenite transformation started at 750°C and finished at 860°C when heated at rate of 5°C/s.

There were two different typical transformation curves during cooling. One was dual-phase transformation, as shown in **Figure 3A**; the other was martensite transformation, shown in **Figure 3B**. In the 0.05°C/s-cooling rate curve, two phases formed: bainite and martensite. The first one started at 740°C and finished at 590°C, while the second started at 420°C and finished at 255°C. However, only martensite formed in the curves when the cooling rate was beyond 1°C/s. Unlike the heating process, the cooling rate did not affect the transformation temperature for either bainite or martensite.

DISCUSSION

The Austenite Formation and Crystal Structure Change

Unlike the martensite transformation, which was fast and caused mainly by lattice distortion and some atom shuffle, the austenite transformation was a long diffusion, nucleation, and growing up journey. Under most circumstances, the martensite shear

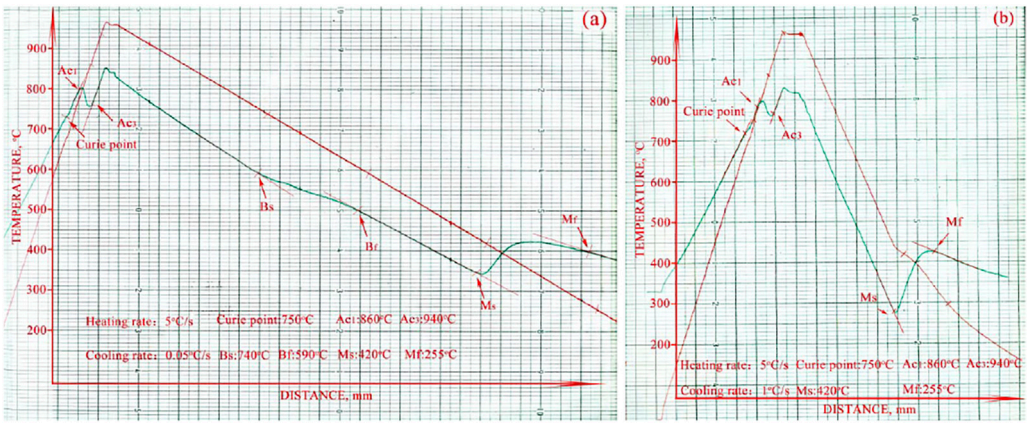

FIGURE 3 | The CCT curves of NSM steel **(A)** 5°C/s heating rate and 0.05°C/s cooling rate, **(B)** 5°C/s heating rate and 1°C/s cooling rate.

transformation from austenite (A→M) was irreversible, unless the heating rate was high enough, beyond 5000°C/s for 0.8C steel for example (Xu, 1999a). That is to say, unlike the M→A, which was only associated with lattice distortion, this transformation involved no diffusion and would finish in seconds, and the austenite transformation from martensite (M→A) of NSM steel showed a series of procedure: martensite degeneration, austenite nucleation, and growing. It could take minutes to complete and even hours to stabilize.

The isothermal holding tests were carried out to test the equilibrium transformation temperature of austenite and its relationship with the Curie point of ferromagnetism.

The diffusivity of carbon, nitrogen, iron, and chromium in BCC iron solvent at 750°C was calculated by the Arrhenius principle as follows (Yong, 2006).

$$D = D_0 \exp\left(\frac{-Q}{RT}\right)$$

Where D = diffusivity, m^2/s.

D_0 = proportionality constant, m^2/s, independent of temperature in range for which the equation is valid.

Q = activation energy of diffusing species, J/mol.

R = molar gas constant = 8.31J/(molK).

T = temperature, K = 1023 K

The results were

$$D_C^{\alpha-Fe} = D_0 \exp\left(\frac{-Q}{RT}\right) = 6.2*10^{-3} * \exp\left(\frac{-80000}{8.31*1023}\right) = 5.1*10^{-12}$$

$$D_N^{\alpha-Fe} = D_0 \exp\left(\frac{-Q}{RT}\right) = 7.8*10^{-3} * \exp\left(\frac{-79100}{8.31*1023}\right) = 7.1*10^{-11}$$

$$D_{Fe}^{\alpha-Fe} = D_0 \exp\left(\frac{-Q}{RT}\right) = 2.1*10^{-4} * \exp\left(\frac{-24100}{8.31*1023}\right) = 5.6*10^{-17}$$

$$D_{Cr}^{\alpha-Fe} = D_0 \exp\left(\frac{-Q}{RT}\right) = 8.5*10^{-3} * \exp\left(\frac{-251000}{8.31*1023}\right) = 8.6*10^{-18}$$

It could be seen that the diffusivity of carbon and nitrogen were about 10^5–10^6 times higher than iron atoms and 10^6–10^7 times higher than chromium atoms. At the same time, the alloy elements that tended to form compounds with carbon and nitrogen had an even lower diffusivity in solid-state diffusion. Their diffusivity in BCC α iron was so very small that it has not yet been detected. However, even in the FCC ϒ iron, taking Nb in 1433 K FCC ϒ iron for an example, the diffusivity could be calculated as

$$D = D_0 \exp\left(\frac{-Q}{RT}\right) = 50.2*10^{-4} * \exp\left(\frac{-252000}{8.31*1433}\right) = 3.2*10^{-12}$$

The diffusivity of Nb at 1433 K was 0.6 times lower than that of carbon at 1023 K. That was why the authors said in the paper that, under the Curie point of ferromagnetism, the microstructure evolution is only associated with the movement of interstitial alloy elements. Therefore, under the Curie point of ferromagnetism, the microstructure evolution only associated with movement of interstitial alloy elements and nucleation of $M_{23}C_6$ particles, shown in **Figure 4A**.

When the temperature reached the Curie point of ferromagnetism (750°C), alloy elements could diffuse efficiently to form $M_{23}C_6$ and MX particles and iron elements could shuffle to change the crystal structure (Zhang et al., 2012), shown in **Figure 4B**. When the temperature was above the Curie point of ferromagnetism, the prior boundary migrated and nucleation of austenite happened, shown in **Figures 4C,D**.

The results indicated that before the nucleation of austenite, the crystal structure already changed into FCC. The austenite nucleation was discovered after isothermal holding for 90min in the NSM steel, although other researchers claimed that the austenite nucleation could take place in less than 15s once the temperature was above Ac1 (Law and Edmonds, 1980). The microstructure observation indicated that the equilibrium austenite transformation for NSM steel started at about 770°C, which was lower than the result of linear expansion curves at 5°C/s heating rate. It could be associated with the transformation hysteresis property.

On the other side, the precipitates, identified as $M_{23}C_6$ and distributing along the boundaries, could retard the boundary migration (Zhang et al., 2019). Although the content of carbon had lowered to under 0.02 wt%, a small number of $M_{23}C_6$

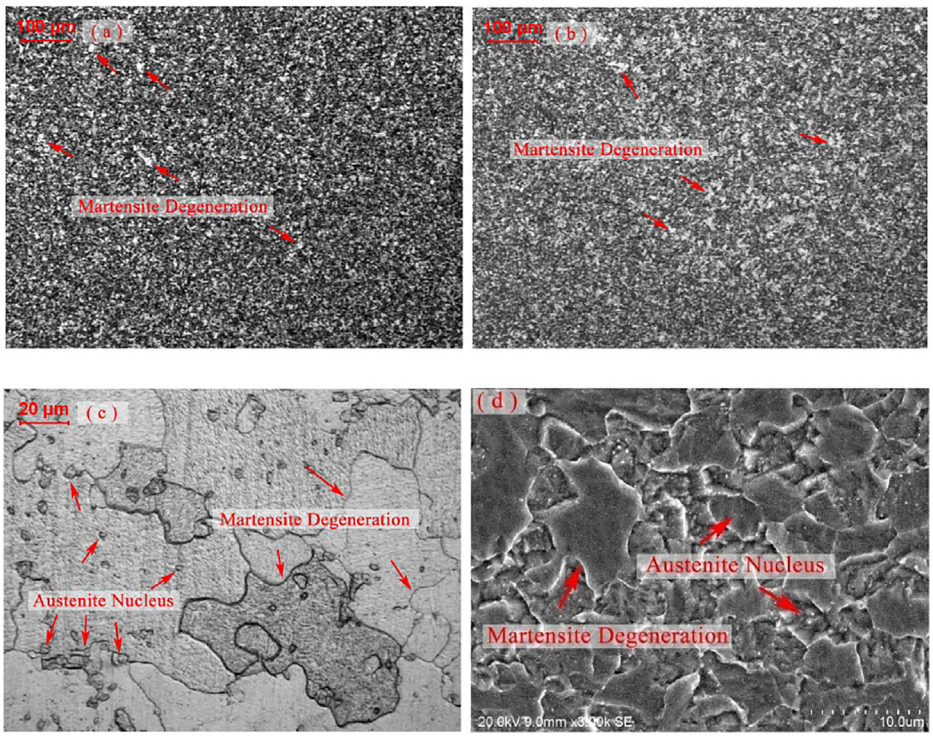

FIGURE 4 | OM/SEM images of NSM steels heated up to **(A)** 700°C, **(B)** 750°C, **(C)** and **(D)** 770°C.

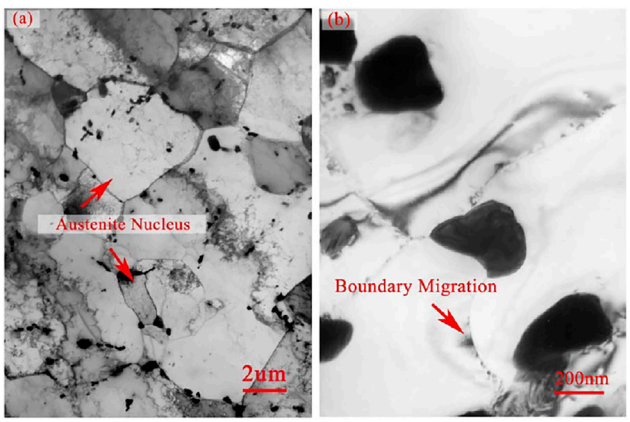

FIGURE 5 | TEM images of NSM steels heated at 770°C for 90 min **(A)** austenite nucleus in degenerated martensite. **(B)** martensite grain boundary migration retarded by the particles.

particles still could be formed. Since the atom number ratio of carbon and nitride approximated 57:100, the particle number ratio of $M_{23}C_6$ and MX would be about 1:10. Furthermore, owing to the nucleation kinetics of $M_{23}C_6$ in this NSM steel, they tend to precipitate together, not distribute separately. The $M_{23}C_6$ particles in NSM steel specimen, isothermal holding at 770°C for 90 min, were detected as shown in **Figure 5B**. They grew to the size of 200–300 nm after this process, which was the optimal size for retarding boundary migration at around 600°C (Zhang et al., 2018). At the same time, the austenite nucleuses were found in the neighbor areas of 200 nm-$M_{23}C_6$, element content of which was shown in **Table 4**, detected by EDS. It could be deduced that some of the M23C6 deposited on the vanadium carbides. With the growth of the austenite grain, the 200 nm-$M_{23}C_6$ lay inside of the new austenite grains rather than along the boundaries, as shown in **Figure 5A**. Therefore, the 200 nm-$M_{23}C_6$ could obstruct the boundary migration and be the austenite nucleus catalyst at the same time.

Although the amount and size of the precipitates were both very small during the continuous heating up of 5°C/s rate, the mechanisms of the microstructure evolution were still employable. Although the precipitation of particles and the boundary migration of martensite microstructure were both martensite degeneration, the first one happened prior to the crystal structure change while the second happened after it. Therefore, the transformation procedure would be reset as follows: formation of intermetallic compound in martensite, crystal structure switch from BCC to FCC, martensite/ferrite grain boundary migration, austenite nucleation, and growing.

The Formation of Carbide-Free Bainite

As is commonly known, the bainite transformation generally happens during isothermal holding. The formation mainly contains two steps: crystal pattern change from FCC to BCC and precipitation. As implied by other researchers, the first step of bainite formation was the same as the formation of ferrite, although the bainite lath substructure could complete the transformation in a speed close to sound velocity. It was close to the formation velocity of

TABLE 4 | Characterization analysis of $M_{23}C_6$ by EDS.

Energy spectrum

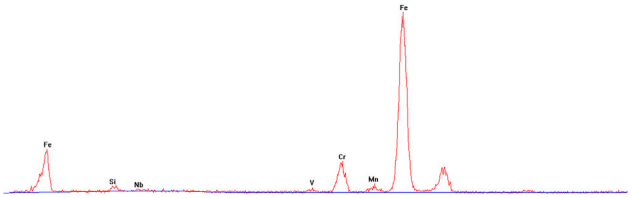

Element content	Element	Si	V	Cr	Mn	Fe	Nb	Total
	Weight %	0.7	1.0	12.2	0.9	84.9	0.4	100.0
Atomic %	1.5	1.1	12.9	0.9	83.5	0.2	100.0	

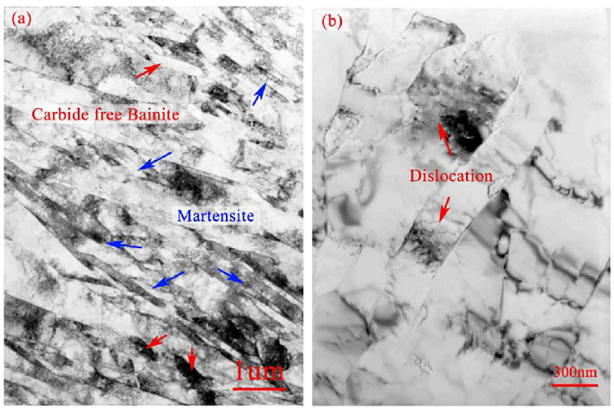

FIGURE 6 | TEM images of NSM steels cooled at 0.1°C/s. **(A)** martensite lath (blue indications) and bainite lath (red indications), **(B)** dislocations in carbide free bainite lath.

martensite (Xu, 1999a). This could also be confirmed in this research by the CCT curve of the heating up progress at 5°C/s. The paper moving speed was 6 cm/min at the heating rate of 5°C/s, and the Curie point transformation last 0.8 cm. Thus, the crystal pattern transformation took 8 s. Therefore, the crystal pattern change could complete in seconds and the long time isothermal holding was only aimed for the intermetallic compound precipitation. However, during the continuous cooling procedure of the NSM steel, the martensite transformation started 2 min after the bainite transformation. It implied that the precipitation only lasted 2 min at 740°C–590°C, which was too short a time and too low a temperature for massive particles to sufficiently precipitate. It was verified by the result of microstructure observation that the particles in bainite microstructure were rare and could only be identified with dislocation nodes, seen in **Figure 6**. Therefore, in this condition, it was recognized as carbide-free bainite, one of the granular bainite type. Unlike martensite, the substructures of bainite, indicated with a red arrow, were single and kept an angle with their primary phases, while the martensite substructures, indicated with a blue arrow, were bunching and parallel.

On the other hand, the martensite transformation occurred after bainite transformation during the cooling process of 0.05°C/s rate. It also indicated that only some of the FCC crystal pattern-microstructure changed into BCC crystal pattern-microstructure, while the rest of them changed during martensite transformation. Therefore, the crystal structure change, either from BCC to FCC or FCC to BCC, was not only concerned with temperature but also bonding with phase transformation. Moreover, during the cooling process at all cooling rates, the crystal pattern change was not detected by CCT curves. Therefore, the crystal structure change from BCC to FCC was sensitive to temperature and could promote the austenite transformation during heating process, while it was not sensitive to temperature but phase transformation when changing from FCC to BCC.

The CCT Diagram

The Critical Rate of Martensite Transformation

The 1°C/s rate-specimen showed single martensite microstructure and the CCT expansion curve of it indicated only martensite transformation, while the 0.1°C/s rate-specimen showed duplex microstructure of martensite and bainite and the CCT expansion curve of it indicated these two-phase transformations. Therefore, neither of these two cooling rates were the critical cooling rate of martensite transformation. To identify the critical cooling rate, another cooling rate of 0.5°C/s test was carried out. The results were shown in **Figure 7**. The CCT expansion curve showed only martensite transformation, yet the microstructure showed a tiny bit of bainite phase. The transformation point detected in the expansion curve was assumed to be the kinetic temperature, while the transformation point detected in microstructure was considered to be the microstructure temperature (Xu and Liu, 1991). Results from these two methods generally remained consistent, especially when a certain amount of bainite was formed. However, when the amount of bainite was very small, the CCT expansion curve was not sensitive enough to detect the transformation. On the other hand, this critical condition was very near the single martensite transformation condition zone. Therefore, the cooling rate of the critical condition could be identified as the critical cooling rate for single martensite transformation.

The Phase Transformation Zones

The results in **Table 5** showed that with the increase of cooling rate, the micro-hardness value increased and kept a constant average value of 313HV since 1°C/s cooling rate. As affirmed by P. V. Yasnii

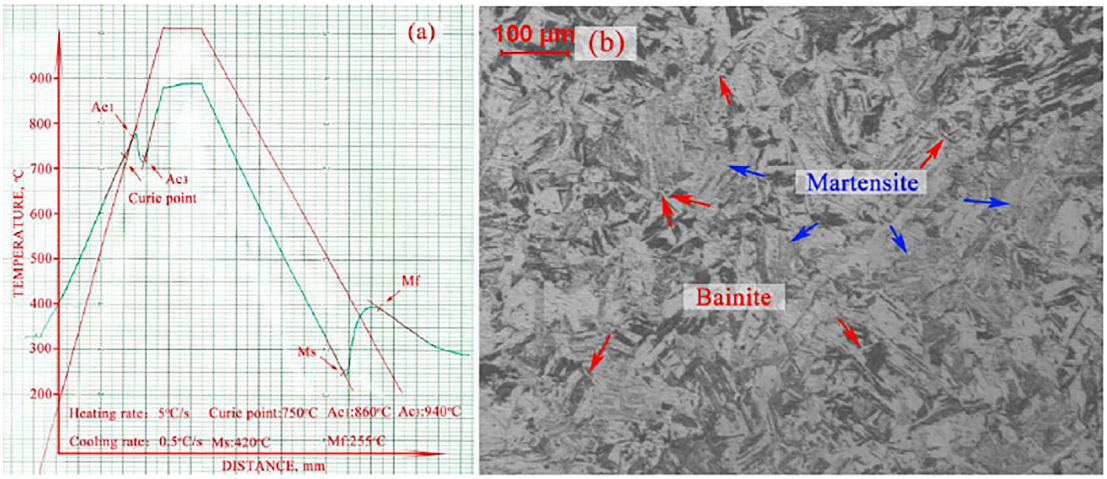

FIGURE 7 | Results of 0.5°C/s cooling rate specimen, **(A)** the CCT expansion curve, **(B)** the microstructure.

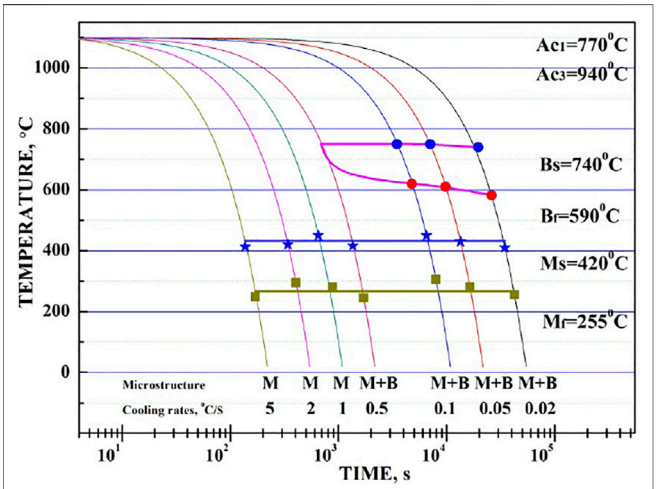

FIGURE 8 | CCT diagram of NSM steel, containing both bainite and martensite transformation when cooled down at a rate below 0.1°C/s, while only martensite transformation when beyond 0.5°C/s.

(Yasnii et al., 2008), the micro-hardness is related to the density of dislocation, and the higher the micro-hardness, the higher the density of dislocation. Therefore, with the microstructure evolution, the micro-hardness would show the difference. Although the microstructure consisted of martensite and bainite at the cooling rate of 0.1°C/s, the micro hardness value achieved 291HV. There was only a 20HV gap to the average value of single martensite microstructure. Therefore, the content of bainite

TABLE 6 | The phase transformation temperatures during different cooling rates.

Cooling rate,°C/s	5	2	1	0.5	0.1	0.05	0.02
B_s	-	-	-	-	739	740	742
B_f	-	-	-	-	585	590	581
M_s	419	419	421	417	421	420	413
M_f	254	257	256	251	252	255	252

microstructure decreased with the increase of cooling rate and it was very rare at 0.1°C/s cooling rate. The micro-hardness of 0.5°C/s cooling rate achieved 300HV, which was very close to the average value and even higher than that of 2 °C/s cooling rate. It confirmed that the content of bainite in the 0.5°C/s cooling rate specimen was less than that in the 0.1°C/s cooling rate. In addition, it substantiated again that the cooling rate of 0.5°C/s could be determined as the critical cooling rate for single martensite transformation.

The CCT diagram of NSM steel, shown in **Figure 8**, was calculated and drawn in logarithm X axis, through the combination of CCT expansion curve, microstructure observation, and micro-hardness tests. It exhibited two phase transformations, bainite and martensite, in the testing cooling rate range. As confirmed by other researchers, the bainite transformation starting temperature maintained a horizontal trend with time parameter (Xu and Liu, 1991), the B_s temperature for NSM steel at 0.5°C/s cooling rate could be assumed to be 710°C the same as the others. Since the critical cooling rate for martensite was defined as 0.5°C/s, the bainite transformation curve would keep a "nose" shape along this cooling curve. Therefore, the finishing temperature of bainite

TABLE 5 | Micro-hardness and microstructure of experiment steel when cooled down at different rates.

Cooling rate, °C/s	5	2	1	0.5	0.1	0.05	0.02
Micro-hardness, HV	312 ± 1.8	299 ± 5.5	319 ± 3.8	300 ± 2.3	291 ± 2.8	229 ± 3.1	192 ± 2.2
Microstructure	M	M	M	M + B	M + B	M + B	M + B

transformation was fit to be around 695°C. The phase transformation points were listed in **Table 6**.

The martensite transformation started at 420°C and finished at 255°C. They both kept a constant value with the cooling rate parameter. It could be confirmed that the martensite transformation was the blast martensite type, which could complete the transformation in seconds.

CONCLUSION

The crystal structure switch from BCC to FCC was sensitive to temperature, which was recognized as the Curie point of ferromagnetism. On the other hand, the crystal structure change from FCC to BCC was only in company with the transformations.

The transformation procedure of austenite in NSM steel was assumed to be as follows: formation of intermetallic compound in martensite, crystal structure change from BCC to FCC, martensite/ferrite grain boundary migration, austenite nucleation, and growing. And the equilibrium austenite transformation was assumed to begin at about 770°C.

During the continuous cooling procedure, the carbide-free bainite would form if the cooling rate was beneath the critical cooling rate. The crystal structure change from FCC to BCC could be completed in seconds and the substructure of it was bainite lath with dislocation nodes.

The cooling rate of 0.5°C/s was defined to be the critical cooling rate for single martensite in NSM steel, according to its inconsistent results of microstructure and CCT expansion curve at this condition.

There were two phase transformation zones in the cooling process of NSM steel, one of which was a nose-shaped bainite zone and the other of which was a stripe-shaped martensite zone.

DATA AVAILABILITY STATEMENT

The original contributions presented in the study are included in the article/Supplementary Material, further inquiries can be directed to the corresponding authors.

AUTHOR CONTRIBUTIONS

WZ was in charge of data analysis and manuscripture writing. WX was in charge of microstructure analysis. PP machined the samples of the steel. JZ observed the microstructure and the tested the microhardness of the steel. YL did the CCT tests. XL analysis the CCT microstructure. YW reveiwed the paper and monitored the data analysis.

FUNDING

This work was financially supported by the Young Scientists Fund (CN), (No. 51601044). Some of the data analysis was also sponsored by Education Department of Guangxi Zhuang Autonomous Region: Microstructure evolution of CLAM steel with polygon prime after EBW, Natural Science Foundation of Guangxi Province (CN), (No. 2015GXNSFBA139225), and the Opening Project of Guangxi Colleges and Universities Key Laboratory of robot and welding.

REFERENCES

Kipelova, A., Kaibyshev, R., and Belyakov, A. (2011). Microstructure Evolution in a 3%Co Modified P911 Heat Resistant Steel under Tempering and Creep Conditions. *Mater. Sci. andEngineering: A* 528, 1280–1286.

Law, N. C., and Edmonds, D. V. (1980). The Formation of Austenite in Low alloy Steels. *Met. Trans.* 11A33, 46.

Rojas, D., Garcia, J., and Prat, O. (2011). 9%Cr Heat Resistant Steels: Alloy Design, Microstructure Evolution and Creep Response at 650°C. *Mater. Sci. Eng. A* 528, 5164–5176.

Sawada, K., Kubo, K., and Abe, F. (2001). Creep Behavior and Stability of MX Precipitates at High Temperature in 9Cr-0.5Mo-1.8W-VNb Steel. *Mater. Sci. Eng. A* 319-321, 784–787. doi:10.1016/s0921-5093(01)00973-x

Speich, G. R., Demarest, V. A., and Miller, R. L. (1981). The Austenite Formation during Critial Annealing in Duplex Steel. *Met. Trans.* 12A, 1.

Tokizane, M., Matsumura, N., and Tsuzaki, K. (1982). The Recrystallization and Austenite Formation of Low Carbon Steel with Deformed Lath Martensite Structure during Heating. *Met. Trans.* 12A, 1.

Wang, H., Yan, W., van Zwaag, S., Shi, Q., Wang, W., Yang, K., et al. (2017). On the 650 °C Thermostability of 9-12Cr Heat Resistant Steels Containing Different Precipitates. *Acta Materialia* 134, 143–154. doi:10.1016/j.actamat.2017.05.069

Xu, Z., and Liu, S. (1991). *The Bainite and its Transformation*. Beijing: The Science Press.

Xu, Z. (1999). *Martensite and its Transformation*. 3 ed. Beijing: The Science Press.

Xu, Z. (1999). *Martensite and Martensite Transformation*. 2 ed. BeiJing: Science Press.

Yasnii, P. V., Marushchak, P. O., Hlad'o, V. B., and Baran, D. Y. (2008). Correlation of the Microdislocation Parameters with the Hardness of Plastically Deformed Heat-Resistant Steels. *Mater. Sci.* 44, 194–200. doi:10.1007/s11003-008-9077-z

Yong, Q. (2006). *Second Phases in Structural Steels*. Beijing: Metallurgical Industry Press.

Zhang, W., Zou, A., and Liu, Y. (2018). A Newly Developed Martensitic Heat Resistant Steel Strengthened by Multi-Sized Carbonitrides. *Mater. Rev. B: Res.* 32, 3606–3627.

Zhang, W.-F., Li, X.-L., Sha, W., Yan, W., Wang, W., Shan, Y.-Y., et al. (2014). Hot Deformation Characteristics of a Nitride Strengthened Martensitic Heat Resistant Steel. *Mater. Sci. Eng. A* 590, 199–208. doi:10.1016/j.msea.2013.10.020

Zhang, W.-F., Sha, W., Yan, W., Wang, W., Shan, Y.-Y., and Yang, K. (2014). Constitutive Modeling, Microstructure Evolution, and Processing Map for a Nitride-Strengthened Heat-Resistant Steel. *J. Materi Eng. Perform.* 23, 3042–3050. doi:10.1007/s11665-014-1026-4

Zhang, W. F., Hu, P., and Zhou, Q. G. (2011). Effect of Heat Treatment on the Mechanical Properties and the Carbide Characteristics of A High Strength Low Alloy Steel. *J. Iron Steel Res. Int.* 18, 143–147.

Zhang, W., Liu, Y., and Liu, X. (2019). Development of Newly Multi-Sized Carbonitrides Strengthened Martensitic Heat Resistant Steel. *Hot Working Tech.* 2019, 48.

Zhang, W., Su, Q., Yan, W., Wang, W., Misra, R. D. K., Shan, Y., et al. (2015). Precipitation Behavior in a Nitride-Strengthened Martensitic Heat Resistant Steel during Hot Deformation. *Mater. Sci. Eng. A* 639, 173–180. doi:10.1016/j.msea.2015.04.101

Zhang, W., Yan, W., Sha, W., Wang, W., Zhou, Q., Shan, Y., et al. (2012). The Impact Toughness of a Nitride-Strengthened Martensitic Heat Resistant

Steel. *Sci. China Technol. Sci.* 55, 1858–1862. doi:10.1007/s11431-012-4903-9

Conflict of Interest: The authors declare that the research was conducted in the absence of any commercial or financial relationships that could be construed as a potential conflict of interest.

Publisher's Note: All claims expressed in this article are solely those of the authors and do not necessarily represent those of their affiliated organizations, or those of the publisher, the editors and the reviewers. Any product that may be evaluated in this article, or claim that may be made by its manufacturer, is not guaranteed or endorsed by the publisher.